FORCED CONVECTION FILM CONDENSATION ON A HORIZONTAL TUBE WITH VARIABLE PROPERTIES

Bodius Salam[1,*], David A. McNeil[2] and Bryce M. Burnside[2] and Sumana Biswas[1]
[1]Department of Mechanical Engineering
Chittagong University of Engineering and Technology, Chittagong-4349, Bangladesh
[2]School of Engineering and Physical Sciences
Heriot-Watt University, Edinburgh, EH14 4AS, UK
*Corresponding email: bsalam@cuet.ac.bd

Abstract: *The paper presents the results of numerical calculations for filmwise condensation of downward flowing pure saturated steam on a horizontal tube. A tube of 19.05 mm diameter was used. Steam approach conditions used were 5000 N/m^2 (T_{sat} = 32.9 ^{o}C) pressure and velocity 5 – 100 m/s. Tube wall temperatures were considered to be constant at 22.9 ^{o}C and 30.9 ^{o}C, giving condensate subcooling ΔT = 10 K and 2 K respectively. Earlier theoretical studies omitted the variations of physical properties with pressure arising from flow of vapor over the tube surface. The present work takes into account these property variations. The velocity and pressure distributions were taken from the potential flow theory. At low condensate subcooling, ΔT = 2 K, and high steam velocities, significant reduction of average heat transfer coefficient was predicted when property variations were taken into account, compared to constant property values. The mean heat flux predicted considering the variation of properties was up to 9% and 42% less than that obtained for ΔT = 10 K and 2 K respectively.*

Keywords: *Laminar filmwise condensation, horizontal tube, boundary layer separation, numerical.*

Nomenclature

d_o	outer diameter, (mm or m)	U_∞	vapor approach velocity (m/s)
H	average condensing heat transfer coefficient (kW/m^{2}K)	u	tangential component of liquid velocity (m/s)
h_θ	local condensing heat transfer coefficient (kW/m^{2}K)	V	transverse component of vapor velocity (m/s)
K	thermal conductivity (W/mK or kW/mK)	v	transverse component of liquid velocity (m/s)
M_{cond}	condensate film mass velocity (kg/m^{2}s)	ΔT_θ	local condensate film temperature difference (K)
p_θ	vapor pressure (mbar or bar)	ΔT	mean condensate film temperature drop (K) = $T_{sat\infty}$-T_w
p_∞	vapor approach pressure (mb or bar)	*Greek symbols*	
q	mean heat flux density based on tube outside wall (kW/m^2)	δ	condensate film thickness (m)
q_θ	local heat flux (kW/m^2)	Δ	vapor boundary layer thickness (m)
r_o	outer radius of the tube (mm or m)	λ	latent heat of vaporization (kJ/kg)
T	temperature (^{o}C)	μ	dynamic viscosity (kg/ms)
T_f	film temperature (^{o}C)	θ	angle measured from front stagnation point
T_{sat}	saturation temperature corresponding to p_θ (^{o}C)	ρ	density (kg/m^3)
$T_{sat\infty}$	saturation temperature corresponding to p_∞ (^{o}C)	τ	shear stress (N/m^2)
T_w	tube wall temperature (^{o}C)	*Subscripts*	
U	tangential component of vapor velocity (m/s)	v	vapor
U_θ	tangential velocity at the edge of vapor boundary layer (m/s)	∞	approach condition
U_δ	tangential velocity at the vapor liquid interface (m/s)	δ	condensate vapor interface
		Properties without subscripts are for condensate film.	

INTRODUCTION

Nusselt[1] is the pioneer of predicting methods for laminar filmwise condensation on horizontal smooth tubes. He considered quiescent vapor. By equating the gravitational and shear forces, Nusselt obtained an expression for film thickness and found the mean condensing heat transfer coefficient,

$$h = C_a\left[\frac{k^3\rho^2 g\lambda}{\mu d_o \Delta T}\right]^{1/4} \quad (1)$$

Nusselt evaluated the coefficient C_a graphically and obtained the value 0.725. A more precise numerical integration yielded $C_a = 0.728$ (Grant[2]). But modern condensers deal with high velocity steam. Vapor velocity creates shear force on the vapor-condensate interface and moreover a pressure gradient is generated in the condensate film. Forced convection condensation on single horizontal tube was analysed numerically by many researchers[3-8]. Shekriladze and Gomelauri[3] considered the shearing stress at the liquid-vapor interface to depend mainly on the momentum transferred by the condensing vapor. They assumed the vapor outside its boundary layer was potential flow. Fujii et al.[4] used two-phase flow and considered equal shear stress in liquid and vapor at the interface. They also considered potential flow outside the vapor boundary layer. Honda and Fujii[5] gave the solution for given conditions of vapor and coolant. The conjunction of the two-phase boundary layer equations and the heat conduction equation within the tube wall was achieved. They considered potential flow and Roshko flow[9], two kinds of flow for distribution of mainstream velocity. Shekriladze and Gomelauri[3], Fujii et al[4]. and Honda and Fujii[5] neglected the pressure gradient in the liquid film, arising from the flow of vapor over the curved surface of the horizontal tube. Rose[6] and Hsu and Yang[8] included the pressure gradient term using the Shekriladze and Gomelauri model of shear stress to see the effect of pressure variation. Karabulut and Ataer[7] also numerically investigated filmwise condensation considering the pressure gradient. They[6,7] showed that when the pressure gradient term was taken into account, the liquid film separation point moved upstream slightly. As none of these studies[6-8] investigated the effect of variation of transport and thermodynamic properties as a result of variation of mainstream pressure, and therefore saturation temperature, due to the flow conditions, it seemed worthwhile to investigate it.

PHYSICAL MODEL AND EQUATIONS

An infinitely long horizontal circular tube is placed in a vertical downward flow of pure saturated steam of free stream velocity U_∞, pressure p_∞ and temperature $T_{sat\infty}$. The vapor condenses on the tube wall maintained at the temperature of T_w which was lower than T_{sat}. The tube wall temperature, T_w, is uniform and T_{sat} varies with pressure. The physical model and the coordinates are shown in Fig. 1. In the formulation of the problem, the following assumptions were made:

(i) The liquid film was laminar.
(ii) The thickness of the liquid film and vapor boundary layer were much smaller than the tube radius r_o.
(iii) The inertia term in the momentum equation and convection term in the energy equation of the liquid film were negligible.
(iv) The radial pressure gradient was negligible.
(v) Surface tension was neglected.
(vi) Thermophysical properties of condensate film were evaluated at T_f, except latent heat of vaporization.
(vii) The tangential velocity at the vapor-liquid interface was much lower than that at the edge of vapor boundary layer.
(viii) The enthalpy given up by vapor was from phase change only.
(ix) A linear temperature profile existed in the condensate layer.
(x) No separation of vapor boundary layer was considered.

The conservation of mass, momentum and energy for the steady laminar layer flow of condensate are described by the following Eqs.(2-4):

$$\frac{\partial u}{\partial x} + \frac{\partial v}{\partial y} = 0 \quad (2)$$

$$\mu\frac{\partial^2 u}{\partial y^2} + (\rho - \rho_v)g\sin\theta - \frac{dp}{r_o\, d\theta} = 0 \quad (3)$$

$$\frac{\partial^2 T}{\partial y^2} = 0 \quad (4)$$

The pressure at the liquid-vapor interface and tangential velocity at the edge of the vapor boundary layer were obtained from potential flow equations for an isolated tube i.e.,

$$p_\theta = p_\infty + \frac{1}{2}\rho_{v\infty}U_\infty^2\left(1 - 4\sin^2\theta\right) \quad (5)$$

$$U_\theta = 2U_\infty\sin\theta \quad (6)$$

The following boundary and compatibility conditions were used,

at the wall (y = 0), $T=T_w$ and $u = v = 0$ (7)

at the liquid-vapor interface ($y = \delta$), $T=T_{sat}$,

$$\tau = \tau_\delta = \mu\frac{\partial u}{\partial y} \text{ and } u_\delta = U_\delta \quad (8)$$

at the edge of vapor boundary layer ($y = \delta+\Delta$),

$$U = U_\theta \quad (9)$$

A heat balance between the heat transferred to the wall surface and heat released by the vapor at the liquid vapor interface by the condensation process gave,

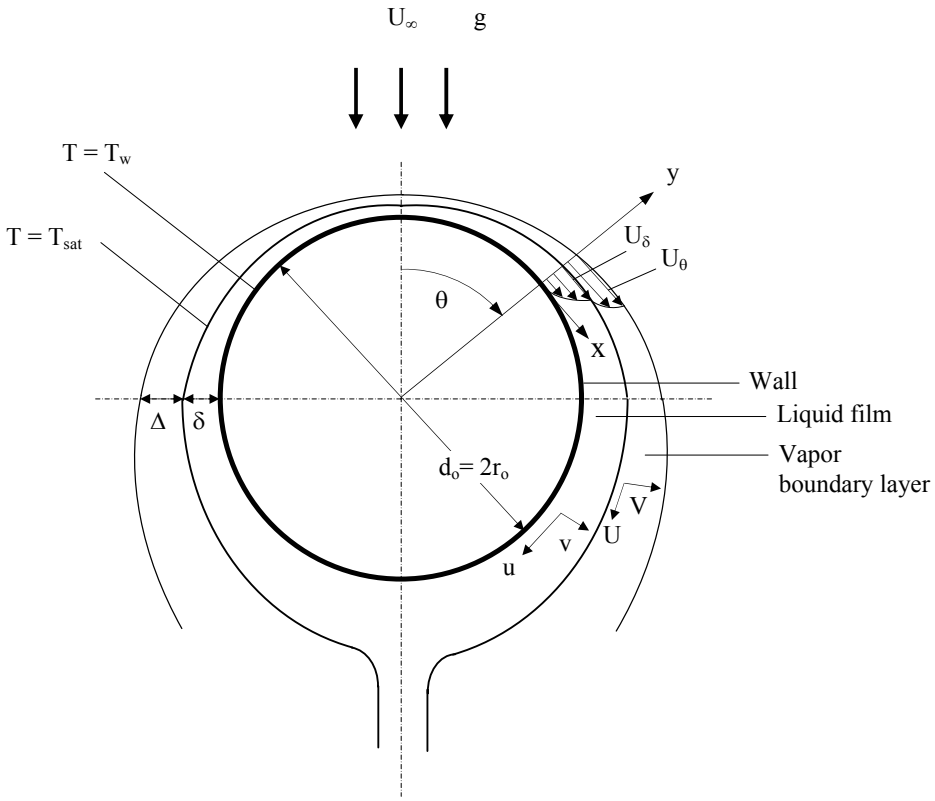

Figure 1. Physical model and the coordinates

$$q = \lambda M_{cond} = k\left(\frac{\partial T}{\partial y}\right)_{y=0} = k\frac{T_{sat} - T_w}{\delta} = \rho\lambda\frac{d}{dx}\int_0^{\delta} udy \tag{10}$$

where M_{cond} was the condensation mass flux.
Intregating Eq. (3) and putting boundary conditions, Eqs. (7) and (8)

$$u = -\frac{(\rho-\rho_v)g\sin\theta\cdot y^2}{2\mu} + \frac{y^2}{2r_o\mu}\frac{dp}{d\theta} + \frac{1}{\mu}\left\{\tau_\delta + (\rho-\rho_v)g\delta\sin\theta - \frac{\delta}{r_o}\frac{dp}{d\theta}\right\}y \tag{11}$$

Shear stress at the liquid-vapor interface, τ_δ, was obtained from the Shekriladze and Gomelauri[3] model, where, for a high condensation rate, the shear stress on the moving film surface mainly depended on the momentum transferred by the condensing mass and was expressed by,

$$\tau_\delta = M_{cond}(U_\theta - U_\delta) \tag{12}$$

Now neglecting U_δ, Eq. (12) was written as,

$$\tau_\delta = M_{cond}U_\theta \tag{13}$$

This model of shear stress had also been used by many other researchers[10,11]. Equations (10) and (11) give,

$$M_{cond} = \frac{k\cdot\Delta T_\theta}{\lambda\delta} = \frac{\rho}{r_o}\frac{d}{d\theta}\int_0^{\delta} udy$$

$$\frac{k\cdot\Delta T_\theta}{\lambda\delta} = \frac{\rho}{r_o}\frac{d}{d\theta}\left[\frac{-(\rho-\rho_v)g\sin\theta\cdot\delta^3}{2\mu\cdot 3} + \frac{\delta^3}{3\cdot 2r_o\mu}\frac{dp}{d\theta} + \frac{1}{\mu}\left\{\tau_\delta + (\rho-\rho_v)g\delta\sin\theta - \frac{\delta}{r_o}\frac{dp}{d\theta}\right\}\frac{\delta^2}{2}\right] \tag{14}$$

where, $\Delta T_\theta = T_{sat}(p_\theta) - T_w$

The properties-pressure relationships for water and vapor[12] between 40 and 60 mb and properties-temperature for water[12] between 20 and 40 ^oC were represented by

$$\left(\frac{T_{sat}}{^oC}\right) = 87.4 - 5.8733333\times10^{-2}\left(\frac{p}{N/m^2}\right) + 1.9566667\times10^{-5}\left(\frac{p}{N/m^2}\right)^2 - 2.66666667\times10^{-9}\left(\frac{p}{N/m^2}\right)^3 + 1.3333333\times10^{-13}\left(\frac{p}{N/m^2}\right)^4$$

$$\left(\frac{\lambda}{J/kg}\right) = 1693000 + 6.3433333\times10^{2}\left(\frac{p}{N/m^2}\right) - 1.9766667\times10^{-1}\left(\frac{p}{N/m^2}\right)^2 + 2.6666667\times10^{-5}\left(\frac{p}{N/m^2}\right)^3 - 1.3333333\times10^{-9}\left(\frac{p}{N/m^2}\right)^4$$

$$\left(\frac{\rho}{kg/m^3}\right) = 996.56 + 6.046667\times10^{-1}\left(\frac{T}{^oC}\right) - 4.08\times10^{-2}\left(\frac{T}{^oC}\right)^2 + 8.933333\times10^{-4}\left(\frac{T}{^oC}\right)^3 - 8\times10^{-6}\left(\frac{T}{^oC}\right)^4$$

$$\left(\frac{\rho_v}{kg/m^3}\right) = 0.035460992$$

$$\left(\frac{\mu}{kg/m.s}\right) = 1.845\times10^{-3} - 6.77833\times10^{-5}\left(\frac{T}{^oC}\right) + 1.775\times10^{-6}\left(\frac{T}{^oC}\right)^2 - 2.86667\times10^{-8}\left(\frac{T}{^oC}\right)^3 + 2\times10^{-10}\left(\frac{T}{^oC}\right)^4$$

$$\left(\frac{k}{W/m.K}\right) = 5.06\times10^{-1} + 1.02833\times10^{-2}\left(\frac{T}{^oC}\right) - 4.18333\times10^{-4}\left(\frac{T}{^oC}\right)^2 + 8.66667\times10^{-6}\left(\frac{T}{^oC}\right)^3 - 6.66667\times10^{-8}\left(\frac{T}{^oC}\right)^4$$

Liquid properties ρ, k, μ were taken at the mean film temperature, T_f, defined[13] as

$$T_f = T_w + 0.33(T_{sat}-T_w)$$

Latent heat of vaporization, λ, was evaluated at the saturation temperature corresponding to the local pressure. Vapor was considered incompressible and density was taken at upstream pressure. Figure 2 shows the pressure at the surface of the condensate film. The with- and without- property variation cases are compared. The pressures are almost identical, pressure at the stagnation point 5080 N/m^2 for variable properties and 5177 N/m^2 for constant properties. In both cases minimum pressure occur at 90^o, 4494 N/m^2 for variable properties and 4468 N/m^2 for constant properties. The results show, even where the velocity is highest, θ = 90^o, there is only 0.1 K difference in temperature between the variable constant property solution. Thus the use of constant vapor density in determining the condensate film surface temperature is justified.

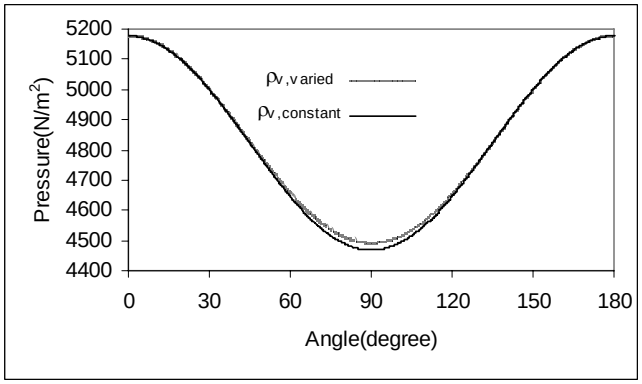

Figure 2. Pressure on condensate film versus angle, U_∞ = 100 m/s

From Eqs. (10), (13), and (14)

$$\Rightarrow \frac{d\delta}{d\theta} = \frac{\frac{k\Delta T_\theta}{\lambda\delta} - \frac{\rho(\rho-\rho_v)g\delta^3\cos\theta}{3r_o\mu} + \left(\frac{\rho\delta^3}{3r_o{}^2\mu}\right)\frac{d^2p}{d\theta^2} - \frac{\rho k\delta\Delta T_\theta}{2r_o\mu\lambda}\frac{dU_\theta}{d\theta} - \frac{\rho kU_\theta\delta}{2r_o\mu\lambda}\frac{d\Delta T_\theta}{d\theta}}{\frac{\rho(\rho-\rho_v)g\delta^2\sin\theta}{r_o\mu} - \left(\frac{\rho\delta^2}{r_o{}^2\mu}\right)\frac{dp}{d\theta} + \frac{\rho k\Delta T_\theta U_\theta}{2r_o\mu\lambda}} \quad (15)$$

Equation (15) was solved numerically using a fourth-order Runge-Kutta method with interval of $\Delta\theta = 0.1^o$. To start the film thickness at $\theta = 0^o$ was required and was obtained from the following condition,

$$\theta = 0,\ \delta = \delta_0, \qquad \frac{d\delta}{d\theta} = 0,\ U_\theta = 0 \quad (16)$$

From Eqs. (15) and (16)

$$0 = \frac{k\cdot\Delta T_\theta}{\lambda\delta_0} - \frac{\rho(\rho-\rho_v)g{\delta_0}^3}{3r_o\mu} + \left(\frac{\rho{\delta_0}^3}{3r_o{}^2\mu}\right)\frac{d^2p}{d\theta^2} - \frac{\rho k\delta_0\Delta T_\theta}{2r_o\mu\lambda}\frac{dU_\theta}{d\theta} \quad (17)$$

Equation (17) was solved for δ_0 by the Newton-Raphson method.

The local heat transfer coefficient was obtained from,

$$h_\theta = \frac{k}{\delta} \quad (18)$$

The local heat flux, $q_\theta = h_\theta(T_{sat} - T_w)$ (19)

The separation of liquid film from the tube wall occurred when the film thickness became infinite and was obtained by the following condition,

$$\frac{d\delta}{d\theta} = \infty, \text{ at } \theta = \theta_c \quad (20)$$

Equations (15) and (20) gave

$$0 = \frac{\rho(\rho-\rho_v)g\delta^2\sin\theta_c}{r_o\mu} - \left(\frac{\rho\delta^2}{r_o{}^2\mu}\right)\frac{dp}{d\theta} + \frac{\rho k\Delta T_\theta U_\theta}{2r_o\mu\lambda} \quad (21)$$

Heat transfer after separation of the liquid film was neglected. Thus the average values of q and h were obtained using the following equations,

$$q = \frac{1}{\pi}\int_0^{\theta_c} q_\theta d\theta \quad (22)$$

$$h = \frac{1}{\pi}\int_0^{\theta_c} h_\theta d\theta \quad (23)$$

The liquid film separation angle was not determined separately. The numerical process was continued until the right hand side value of Eq. (21) changed the sign. This situation happened when θ reached θ_c.

NUMERICAL MODELS STUDIED

The numerical model described, Model B, was compared to Model A, described by Rose[6]. This is identical except that the thermo-physical properties were considered constant at the value pertaining to the saturation temperature of the upstream flow at pressure p_∞. Both models assumed potential flow of the vapor around the tube. In model B the thermo-physical properties varied with pressure, p_θ, Eq. (5).

RESULTS AND DISCUSSION

The filmwise condensation of saturated steam at an approach pressure 50 mbar and temperature of 32.9 ^{o}C was considered. Tube wall temperatures were 22.9 ^{o}C and 30.9 ^{o}C, which gave condensate film temperature drops, ΔT, 10 K and 2 K respectively. 10 K condensate film temperature drop was chosen as the maximum practical value corresponding to an overall temperature drop (steam to coolant) of 15 K, considering minimum thermal resistance in the coolant side and negligible thermal resistance of the tube wall. The calculations were carried for range of vapor approach velocities, U_∞, from 5 to 100 m/s. Tube outside diameter was considered to be 19.05 mm.

Figure 3 shows the effect of vapor velocity on film thickness for ΔT = 2 K. At 5 m/s for both models A and B the liquid films separated at 180^o. At 50 m/s separation occurred for model A at 129.6^o and for model B at 127.1^o. At 100 m/s the liquid film separations occurred even earlier at 122.6^o for model A and at 93.8^o for model B. Using the variable properties model, separation of the liquid film occurred earlier than for the constant properties model. For both the models, the high velocity vapor drag on the condensate on the front part of the tube caused the film thickness to be low. Film separation occurred earlier when property variation was allowed for than when it was not. Figure 4 shows the effect of vapor velocity on film thickness for ΔT = 10 K. In the case of both models A and B the condensate film separated further round the tube when ΔT = 10 K than when ΔT = 2 K. This is attributed to higher suction at higher ΔT. Like before, model B exhibited little earlier separation than model A.

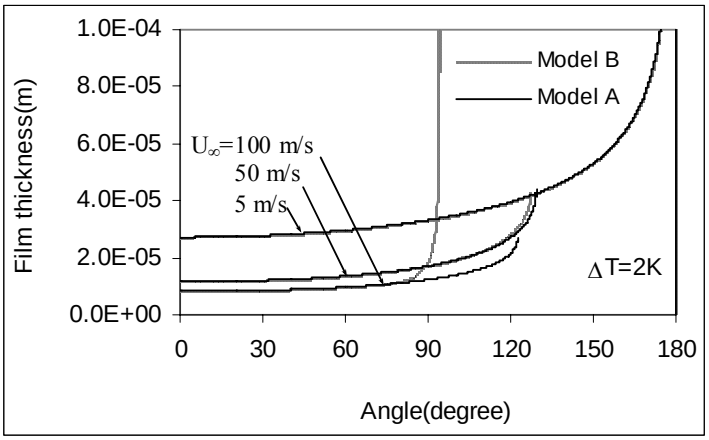

Figure 3. Effect of vapor approach velocity on film thickness for $\Delta T = 2$ K

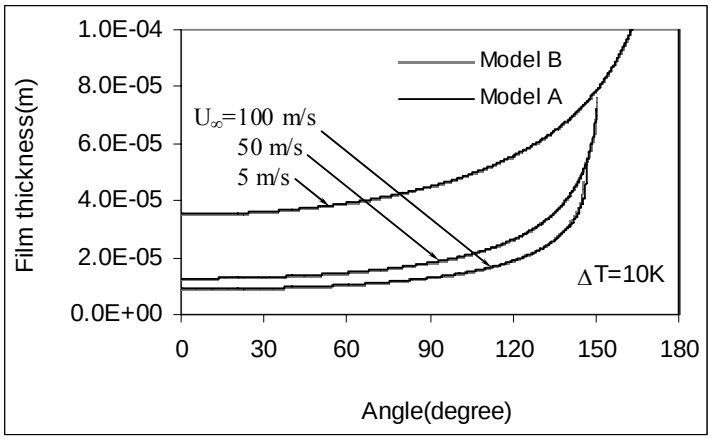

Figure 4. Effect of vapor approach velocity on film thickness for $\Delta T = 10$ K

Figures 5 and 6 show the effect of vapor velocity on local heat transfer coefficients for $\Delta T = 2$ K and 10 K. Increase of velocity showed increased heat transfer coefficient for thinner film thickness. Model B shows little difference from model A up to the separation point. At very high velocity because of earlier separation the heat transfer coefficient fell to zero. Because of saturation temperature variation with pressure, the maximum T_{sat} was 33.5 ^oC at the front stagnation point and a minimum of 30.9 ^oC at 90^o from the front stagnation point when $U_\infty = 100$ m/s. And at this extreme condition the maximum variation of thermal conductivity was only 0.2%. Because of this, the local heat transfer coefficient strongly depended on film thickness.

Figures 7 and 8 show the local heat flux variations for $\Delta T = 2$ K and 10 K respectively. At a vapor velocity of 5 m/s properties variations with pressure (model B) made no significant difference to heat flux relative to the constant property model (A). No significant difference in ΔT_θ, Fig. 9, was responsible for this. At 50 m/s approach velocity, a minor difference in heat flux distribution was observed between model A and B for $\Delta T = 10$ K. For $\Delta T = 2$ K, the difference was significant between models A and B. After separation of the condensate film boundary layer no heat transfer was postulated. At 100 m/s approach velocity for $\Delta T = 2$K, the local ΔT value fell to 0 K at 84.5^o angle. When saturation temperature fell equal to the wall temperature value, no heat transfer was considered further round the tube, although liquid film separation occurred at 93.8^o.

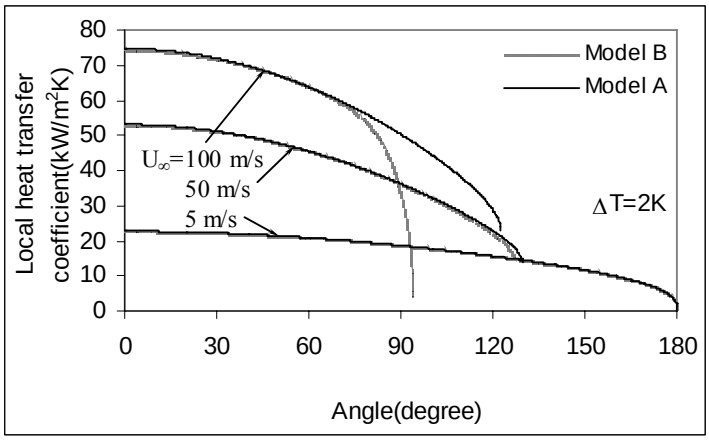

Figure 5. Effect of vapor approach velocity on local heat transfer coefficient for ΔT = 2K

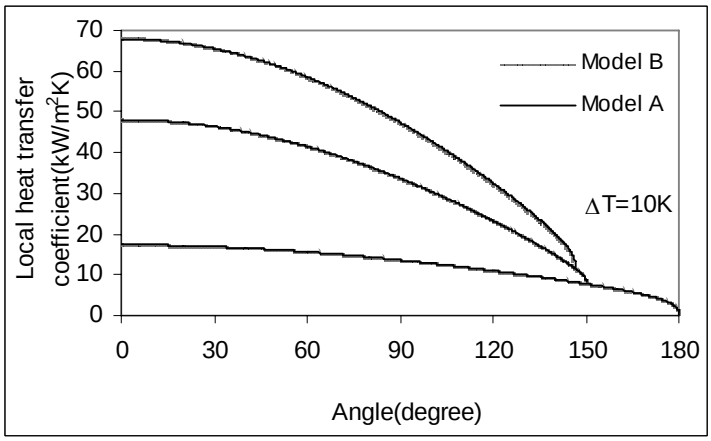

Figure 6. Effect of vapor approach velocity on local heat transfer coefficient for ΔT=10K

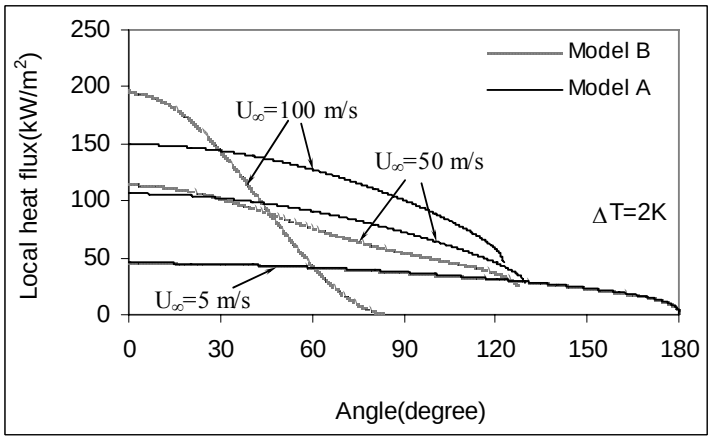

Figure 7. Effect of vapor approach velocity on local heat flux for ΔT = 2 K

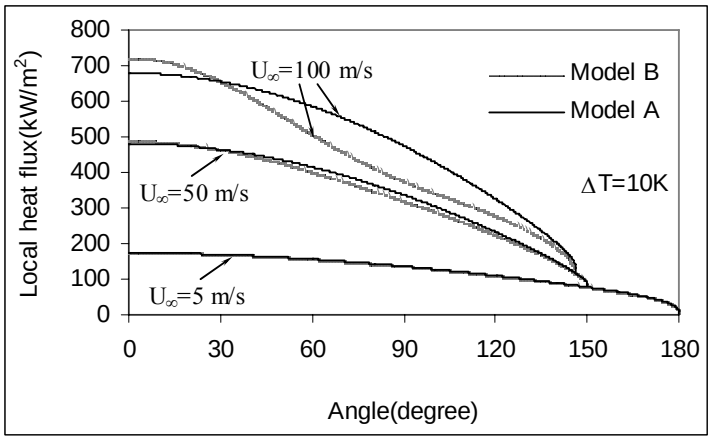

Figure 8. Effect of vapor approach velocity on local heat flux for ΔT = 10 K

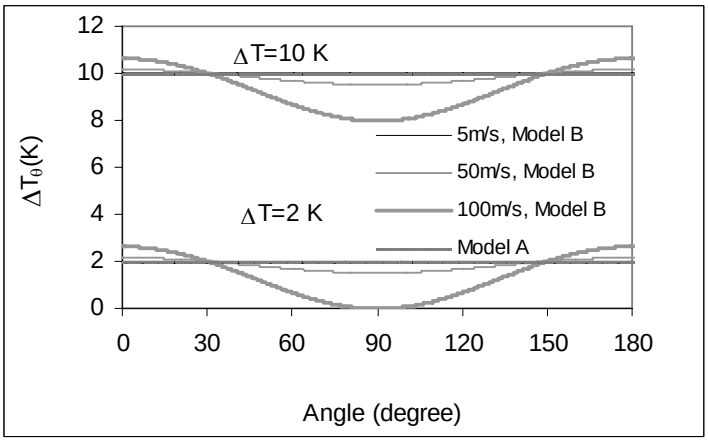

Figure 9. Effect of vapor approach velocity on local condensate film temperature drop

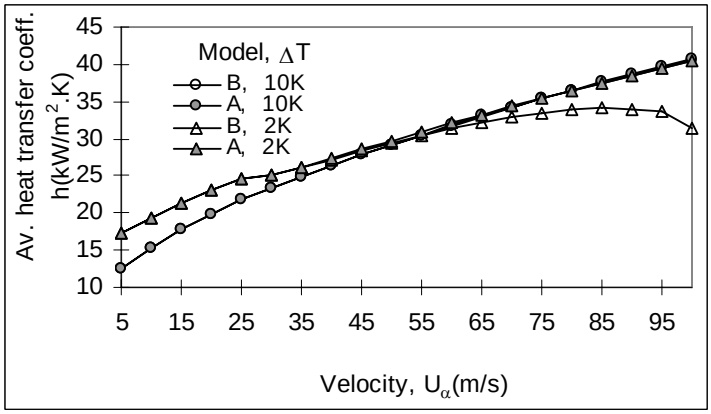

Figure 10. Effect of vapor approach velocity on average heat transfer coefficient

Figure 10 shows the effect of approach velocity on average heat transfer coefficient for both the models. For ΔT = 10 K, the average heat transfer coefficient increased with increase of velocity. No significant difference was observed between the average heat transfer coefficient obtained using the

properties variable model (B). The maximum reduction of heat transfer coefficient was around 0.6% at 100 m/s when failing to take into account the variation in thermodynamic and transport properties. For ΔT = 2 K, when property variation was not considered (model A), the average heat transfer coefficient increased with increase of approach velocity. However when properties variation was considered (model B), above 85 m/s the average heat transfer coefficient decreased with increase in velocity. Up to 45 m/s the difference between h values obtained from the two models was insignificant. Above 45 m/s, the decrease in h using model B was greater, with a maximum reduction of 22%, compared to model A, at 100 m/s. Earlier separation of condensate film for lower momentum because of lower condensation rate was responsible for this, Fig. 11. Figure 10 shows that up to 40 m/s the average heat transfer coefficient values for ΔT = 10 K were lower than for ΔT = 2 K. This was because of the thicker condensate film ΔT = 10 K, and no separation up to 25 m/s. Consequently, the average heat transfer coefficient values all over the tube were lower than when ΔT = 2 K. Above 25 m/s the thicker film was the dominant effect on heat transfer rather than the delay in separation. But at velocities higher than 50 m/s, for ΔT = 2 K earlier separation for model B was responsible for rapid thickening of the condensate film and rapid reduction of local heat transfer coefficient values before separation (Fig. 12) and consequent reduction of average heat transfer coefficient.

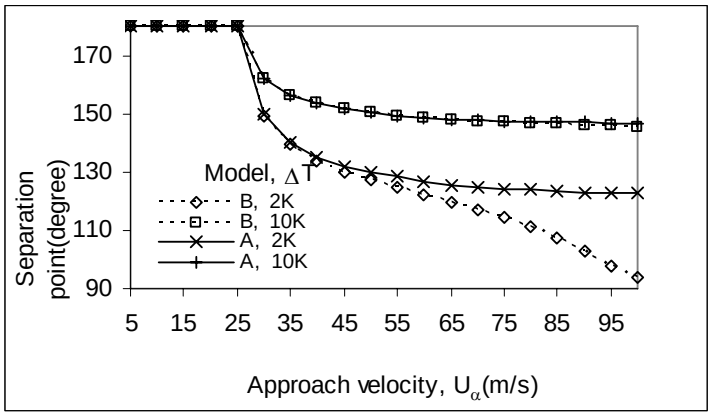

Figure 11. Effect of vapor approach velocity on condensate film separation point

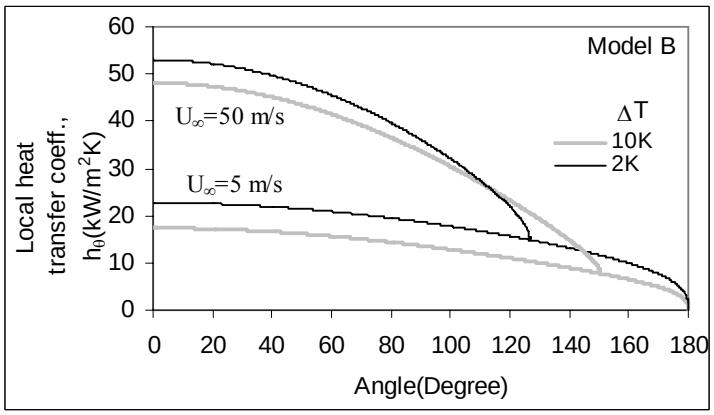

Figure 12. Effect of ΔT and U_∞ on heat transfer coefficient variation

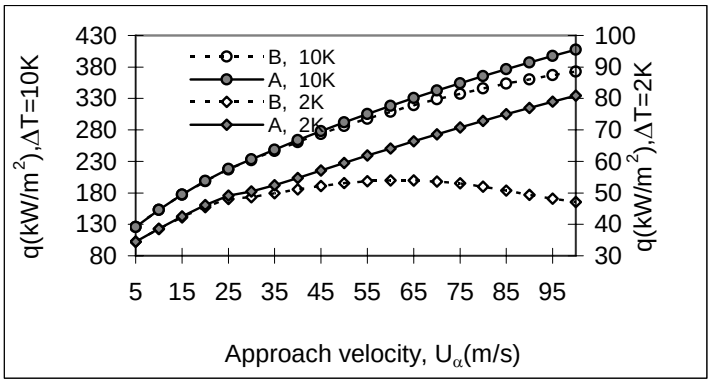

Figure 13. Effect of approach velocity on heat flux

Figure 13 shows the effect of velocity on average heat flux. Considering the properties variations, the average heat fluxes were found to be lower than constant property model values. For ΔT = 10 K, the average heat flux increased with the increase of velocity for both the models. At 5 m/s the reduction was negligible and at 100 m/s, it was 8.6%. The main reason for this reduction was the variation of condensate subcooling (ΔT) (Fig. 9) because of variation of saturation temperature with pressure. For ΔT = 2 K, the average heat flux predicted by model A had a similar increasing trend with velocity for model A. But for the property variation model (B) the average heat flux increased up to 60 m/s and decreased above that. The effect of earlier separation, Fig. 10, and ΔT_θ variation were responsible for this. At 5 m/s the reduction of heat flux, q, predicted by model B was 0.1% but increased to 41.8% at U_∞ = 100 m/s.

CONCLUSIONS

Filmwise condensation of downward flowing saturated pure steam on a horizontal tube was investigated numerically. The numerical technique used was based on the assumption of Rose[6], but properties were varied with pressure (model B). The velocity and pressure distributions around the tube were taken from the single isolated tube potential flow theory, as was done by Rose. The average condensing heat transfer coefficient obtained including the variation of properties with pressure (model B) under predicted the values of model A by up to 0.6% and 22% for ΔT = 10 K and 2 K respectively. The mean heat flux obtained considering the variation of properties with pressure under predicted the values of model A by up to 8.6% and 41.8% for ΔT = 10 K and 2 K respectively. Due to the dominating effect of liquid film separation on heat transfer, the average heat flux decreased above U_∞ = 60 m/s for ΔT = 2 K. For condensate subcooling lower than 2 K and/or approach velocity higher than 100 m/s, heating of the steam would occur on part of the tube because of the negative local ΔT value. Further numerical investigation of this problem is required to consider the conjugate problem of heat transfer in the condenser tube and in the condensate film.

REFERENCES

[1] Nusselt, W., 1916, Die Oberflächenkondensation des Wasserdampfes (The Surface Condensation of Water Vapour), *Zeitschrift des Vereines Deutscher Ingenieure*, 60, 541-546, and 569-575.

[2] Grant, I. D. R., 1972, Film Condensation of Pure Vapours, *National Engineering Laboratory,* Glasgow, Paper No. 2.

[3] Shekriladze, I. G. and Gomelauri, V. I., 1966, Theoretical Study of Laminar Film Condensation of Flowing Vapour, *Int. J. Heat Mass Transfer*, 9, 581-591.

[4] Fujii, T., Uehara, H. and Kurata, C., 1972, Laminar Filmwise Condensation of Flowing Vapour on a Horizontal Cylinder, *Int. J. Heat Mass Transfer*, 15, 235-246.

[5] Honda, H. and Fujii, T., 1984, Condensation of Flowing Vapor on a Horizontal Tube-Numerical Analysis as a Conjugate Heat Transfer Problem, *Trans. ASME, J. Heat Transfer*, 106, 841-848.

[6] Rose, J. W., 1984, Effect of Pressure Gradient in Forced Convection Film Condensation on a Horizontal Tube, *Int. J. Heat Mass Transfer*, 27, 39-47.

[7] Karabulut, H. and Ataer, Ö. E., 1996, Numerical Analysis of Laminar Film-wise Condensation, *Int. J. Refrig.,* 19(2), 117-123.

[8] Hsu, C.-H., Yang, S.-A., 1999, Pressure Gradient and Variable Wall Temperature Effects During Filmwise Condensation from Downward Flowing Vapors onto a Horizontal Tube, *Int. J. Heat Mass Transfer*, 42, 2419-2426.

[9] Roshko, A., 1954, A New Hodograph for Free-Stream-Line Theory, NACA TN 3168.

[10] Memory, S. B., Lee, W. C. and Rose, J. W., 1993, Forced Convection Film Condensation on a Horizontal Tube-Effect of Surface

Temperature Variation, *Int. J. Heat Mass Transfer*, 36, 1671-1676.

[11] Memory, S. B. and Rose, J. W., 1994, Effect of Variable Viscosity in the Presence of Variable Wall Temperature on Condensation on a Horizontal Tube, *Int. J. Heat Mass Transfer*,37, 2321-2326.

[12] Rogers, G. F. C. and Mayhew, Y. R., 1995, Thermodynamic and Transport Properties of Fluids, 5th edition, Blackwell, Oxford.

[13] Denny, V. E. and Mills, A. F., 1969, Laminar Film Condensation of a flowing Vapor on a Horizontal Cylinder at Normal Gravity, *Trans. ASME, J. Heat Transfer*, 495-501.